Ann. Occup. Hyg., Vol. 55, No. 8, pp. 841–864, 2011

doi:10.1093/annhyg/mer075

A Generic, Cross-Chemical Predictive PBTK Model with Multiple Entry Routes Running as Application in MS Excel; Design of the Model and Comparison of Predictions with Experimental Results

FRANS J. JONGENEELEN[1]* and WIL F. TEN BERGE[2]

[1]IndusTox Consult, PO Box 31070, NL-6503 CB Nijmegen, the Netherlands; [2]Santoxar, Wolter Visscherstraat 40, NL-6931 CV Westervoort, the Netherlands

Received 21 December 2010; in final form 8 August 2011

Aim: Physiologically based toxicokinetic (PBTK) models are computational tools, which simulate the absorption, distribution, metabolism, and excretion of chemicals. The purpose of this study was to develop a physiologically based pharmacokinetic (PBPK) model with a high level of transparency. The model should be able to predict blood and urine concentrations of environmental chemicals and metabolites, given a certain environmental or occupational exposure scenario.

Model: The model refers to a reference human of 70 kg. The partition coefficients of the parent compound and its metabolites (blood:air and tissue:blood partition coefficients of 11 organs) are estimated by means of quantitative structure–property relationship, in which five easily available physicochemical properties of the compound are the independent parameters. The model gives a prediction of the fate of the compound, based on easily available chemical properties; therefore, it can be applied as a generic model applicable to multiple compounds. Three routes of uptake are considered (inhalation, dermal, and/or oral) as well as two built-in exercise levels (at rest and at light work). Dermal uptake is estimated by the use of a dermal diffusion-based module that considers dermal deposition rate and duration of deposition. Moreover, evaporation during skin contact is fully accounted for and related to the volatility of the substance. Saturable metabolism according to Michaelis–Menten kinetics can be modelled in any of 11 organs/tissues or in liver only. Renal tubular resorption is based on a built-in algorithm, dependent on the (log) octanol:water partition coefficient. Enterohepatic circulation is optional at a user-defined rate. The generic PBTK model is available as a spreadsheet application in MS Excel. The differential equations of the model are programmed in Visual Basic. Output is presented as numerical listing over time in tabular form and in graphs. The MS Excel application of the PBTK model is available as freeware.

Experimental: The accuracy of the model prediction is illustrated by simulating experimental observations. Published experimental inhalation and dermal exposure studies on a series of different chemicals (pyrene, *N*-methyl-pyrrolidone, methyl-tert-butylether, heptane, 2-butoxyethanol, and ethanol) were selected to compare the observed data with the model-simulated data. The examples show that the model-predicted concentrations in blood and/or urine after inhalation and/or transdermal uptake have an accuracy of within an order of magnitude.

Conclusions: It is advocated that this PBTK model, called IndusChemFate, is suitable for 'first tier assessments' and for early explorations of the fate of chemicals and/or metabolites in the human body. The availability of a simple model with a minimum burden of input information on the parent compound and its metabolites might be a stimulation to apply PBTK modelling more often in the field of biomonitoring and exposure science.

Keywords: biomarker of exposure; blood; body burden; internal exposure; PBTK-model; prediction, urine

*Author to whom correspondence should be addressed.
Tel: +31243528842; fax: 3124350090;
e-mail: frans.jongeneelen@industox.nl

INTRODUCTION

A physiologically based toxicokinetic (PBTK) or physiologically based pharmacokinetic (PBPK) model is an structural mathematical model, comprising the tissues and organs of the body with each perfused by, and connected via, the blood circulatory system. Such models are computational tools that can refine the assessment of the fate of chemicals in the body by simulation. In PBTK models, the body is subdivided into anatomical compartments representing individual organs or tissue groups. The transport of chemical in the body is described by mass balance differential equations that incorporate blood flows, partitioning into compartments and tissue volumes. After incorporation of elimination processes like metabolism and excretion, the fate and disposition of the parent chemical and metabolites can be predicted and extrapolated. Most PBPK models are chemical specific. Often, they are built for very specific purposes, for example, the estimation of disposition of a certain drug prior to *in vivo* studies (Yu and Amidon, 1999; Poulin and Theil, 2002) or cancer risk assessment for a specific industrial chemical (Krewski *et al.*, 1994; Clewell *et al.*, 2000, 2001). Industrial chemicals are generally less extensive studied in comparison with medicines considering absorption, distribution, metabolism, and excretion (ADME). For pharmaceutical agents, ~50 PBPK models are commercially available (van de Waterbeemd and Gifford, 2003).

Several initiatives were taken to develop PBPK models that can be used for industrial compounds (Haddad *et al.*, 1999, 2000; Tardif *et al.*, 2002; Kim *et al.*, 2007). Cahill *et al.* (2003) published a generic PBPK model for multiple environmental contaminants in MS Excel. The model relies on available physical–chemical partitioning and reactivity data and experimental partitioning and absorption efficiency data can also be used to refine the parameters. The model can be applied for various chemicals and exposure regimes with only the physical–chemical properties, reaction rates, and exposure conditions being variables. However, estimation of urinary concentrations was not part of the model. Luecke *et al.* (2008) reported on a generalized PBPK model (called PostNatal) that could be used by supplying appropriate pharmacokinetic parameter estimates for the chemicals of interest. The MS Windows program consists of four PBPK models in one with each PBPK model acting independently or totally integrated with the others through metabolism by first order or Michaelis–Menten kinetics. Dosing may occur by ingestion, dermal, inhalation, or more. Elimination can be modelled through the faeces, urine, and/or hair. Beliveau and Krishnan (2005) developed a PBPK spreadsheet program in MS Excel for the inhalation of volatile organic compounds (VOC). It is driven by a quantitative–structure property relationship (QSPR) that they derived from experimental rat data, based on structural fragments (Beliveau *et al.*, 2005). US-EPA also developed a very detailed generic PBPK model, the so-called Exposure Related Dose Estimating Model, focusing on risk assessment for environmental agents (US-EPA, 2006). It allows the user to input data up to a very high level of detail. Disadvantage of the model is that compound-specific data are needed. Other generalized PBPK models are Poulin and Theil (2002) (focused to drug discovery prior to *in vivo* studies), PKQuest by Levitt (2002) (focused to comparisons between animals and man), PKSim by Willmann *et al.* (2005) (focused on pharmaceutical agents), and a generic PBPK model by Brightman *et al.* (2006) (predicting plasma concentrations based on extrapolation of animal data).

The aim of this study was to develop a PBTK model as a screening tool for new data-poor chemicals related to exposure of workers and/or consumers to do early explorations of the ADME of chemicals following inhalation and dermal exposure. The tool should have a high level of transparency and should run with a minimum of input data. The resulting PBTK model should be a generic tool, thus being able to estimate blood and urine concentrations of various chemicals, given a certain exposure scenario. Early work of Johanson (1986) describes the programming of physiologically based models in a spreadsheet. Haddad *et al.* (1996) showed that a PBPK model constructed in MS Excel provides the same results as a PBPK model in commercial available software. This paper extends such an approach, where the differential equations of the physiological model are solved by means of an MS Excel macro instruction using Visual Basic.

Partitioning between blood:air and between tissue:blood is related to easy available physical–chemical properties. The relationships were worked out into QSPRs, which algorithms have been incorporated into the PBTK model.

A novel dermal uptake module has been added to the PBTK model. Also, serial metabolism and urinary excretion have been incorporated in the model.

This paper describes the resulting model, called IndusChemFate. The accuracy of predictions of the PBTK model IndusChemFate has been tested. Six studies with different exposure scenarios (inhaled concentration and dermal dose rate) to different

chemicals and repeatedly measured concentration in blood and/or urine were selected to compare the experimentally measured levels with the results of the IndusChemFate model simulation.

THE GENERIC PBTK MODEL

PBTK models comprise four main types of parameters: (i) physiological, (ii) anatomical, (iii) biochemical, (iv) physicochemical. Physiological and anatomical parameters include tissue masses and blood perfusion rates, estimates of cardiac output, and alveolar ventilation rates. Biochemical parameters include metabolic rates. Physicochemical parameters refer to e.g. octanol–water partition coefficient, vapour pressure, molecular weight, solubility, and density. The layout of the PBTK model is presented in Fig. 1. The model contains 11 body compartments [lung, heart, brain, skin, adipose, muscles, bone, bone marrow, stomach and intestines (lumped), liver, and kidney]. The model assumes a reference human of 70 kg.

The human physiological parameters such as organ volumes, blood flows, cardiac output, and alveolar ventilation are adopted from Technical Guidance Documents of REACH (ECHA, 2008a, b) and are presented in Table 1.

MS Excel is a commonly used spreadsheet program and has been considered as the most user-friendly software platform for the model. The data handling proceeds via input and output cells. Stepwise numerical integration routine according to Euler can be entered. The integration intervals can be set. Minimum is an integration interval of 1000 steps h^{-1}, best results are found at 10 000 steps h^{-1}.

Prediction of partitioning of chemicals

A partition coefficient is the ratio of the concentration of a chemical between two phases in thermodynamic equilibrium. The tissue:blood partition coefficients are relevant for simulation of the distribution in the body. The blood:air partition coefficient controls the uptake of a compound in the alveoli. A novel QSPR to estimate the blood:air partition coefficient has been derived. A wide range of VOCs with measured blood:-air values for humans from many sources were reported in the paper of Meulenberg and Vijverberg (2000). Of 137 VOCs with human partitioning data, 106 compounds had experimentally measured values for the partition coefficient blood:air. Initial analyses with selected substances ($n = 106$) showed that this group consisted of as two homogeneous groups with similar properties: a group of very water soluble and volatile substances with a vapour pressure >4000 Pa and

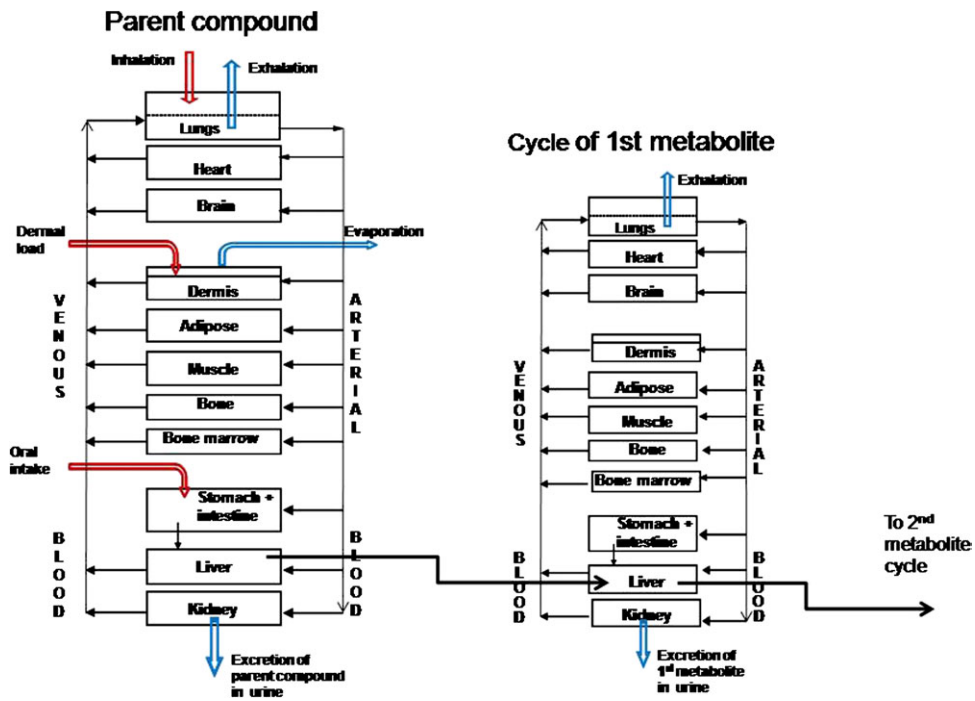

Fig. 1. The outline of the PBPK model as applied in the IndusChemFate PBTK model tool.

Table 1. The human physiological parameters of the PBTK model

Parameter	Symbol	At rest	Light work
Cardiac output (l h^{-1})	CardOutp	390	640
Alveolar ventilation (l h^{-1})	AlvVent	530	1350
Fraction of cardiac output to adipose tissue	FrAdip	0.053	0.0417
Fraction of cardiac output to bone tissue	FrBone	0.021	0.0128
Fraction of cardiac output to brain tissue	FrBrain	0.12	0.0731
Fraction of cardiac output to heart tissue	FrHeart	0.053	0.053
Fraction of cardiac output to kidney tissue	FrKidney	0.215	0.131
Fraction of cardiac output to liver venous	FrLivVen	0.215	0.131
Fraction of cardiac output to liver arterial	FrLivArt	0.053	0.0566
Fraction of cardiac output to lung tissue	FrLung	0.03	0.03
Fraction of cardiac output to muscle tissue	FrMuscle	0.15	0.3826
Fraction of cardiac output to skin tissue	FrSkin	0.05	0.05
Fraction of cardiac output to bone marrow	FrMarrow	0.04	0.0381

a dimensionless Henry coefficient of >0.1 (n = 49) and the group of other substances not meeting these criteria (n = 57). The dimensionless Henry coefficient (Henry-DL) and the octanol:air partition coefficient (K_{oa}) were retrieved as measured values from US-EPA EPIsuite 4.0 database. For both subsets, a multiple regression analysis (as y = intercept + ax + bz) was conducted with the reciprocal dimensionless Henry coefficient and the octanol:water partition coefficient asindependent variables (x and z) and the blood:air partition coefficient as dependant variable (y). This resulted in two separate regression formulas 1 and 2:

$$\begin{aligned} &\textit{In case of substance with a vapour pressure} > 4000 \textit{ Pa and a dimensionless Henry coefficient} > 0.1 \quad \textit{Blood : air partition coefficient} \\ &= 0.8417/\mathrm{HenryDL} + 0.006232 \times K_{oa}\,(N = 49, R^2 = 0.87) \end{aligned} \tag{1}$$

$$\textit{Other substances} \quad \textit{Blood : air partition coefficient} = 0.4445/\textit{Henry}\text{–DL} + 0.005189 \times K_{oa}.\ (N = 57\ ,\ R^2 = 0.99) \tag{2}$$

A plot of experimental human partition coefficients blood:air and QSPR estimated values is presented in Fig. 2. Ninety estimates of the 106 experimental partition coefficients were within a factor 2 and 99 were within a factor 3 of the experimental results. In order to limit the necessary entry data of physical–chemical properties of substances under study, additional algorithms were added to the MS Excel application to calculate the dimensionless log Henry coefficient and the octanol:air partition coefficient from basic physical–chemical properties. The Henry coefficient is in the program derived from the vapour pressure, molecular weight, water solubility, gas constant, and temperature according to equation 3. The octanol:air partition coefficient (K_{oa}) is calculated from the octanol:water partition coefficient (K_{ow}) and the Henry coefficient-dimensionless using equation 4:

$$\begin{aligned} \text{Henry–DL} = {} & \text{Vapour pressure} \times \\ & \text{molecular weight}/(\text{water solubility} \times \\ & \text{gas constant} \times \text{temperature°K}) \end{aligned} \tag{3}$$

$$\log(K_{oa}) = \log(K_{ow}) - \log(\text{Henry–DL}) \tag{4}$$

For the blood:tissue partitioning, the QSPR algorithm as described by DeJongh *et al.* (1997) has been applied. They describe the distribution of compounds between blood and human body tissues as a function of water and lipid content of tissues and the n-octanol:water partition coefficient (K_{ow}). Experimental octanol:water partition coefficients of the 24 compounds were used for calibration of the model for human tissue–blood partition coefficients. As DeJongh *et al.* presented algorithms for only five tissue types and the IndusChemFate model consists of 11 tissue compartments, some compartments of the model share the same partitioning algorithm (see Table 2). This selection is based on the lipid fraction of the tissue (Woodard and White, 1986).

As an example, the algorithm for the brain:blood partition coefficient is shown as formula 5.

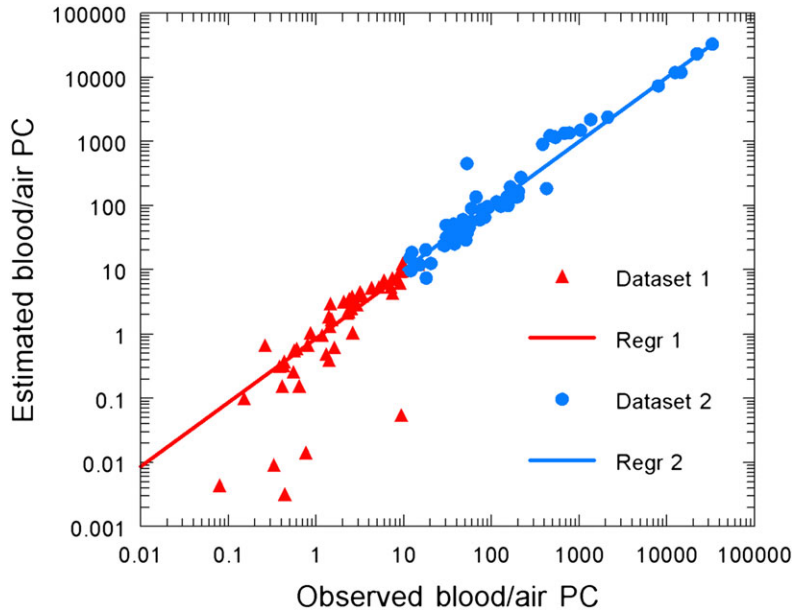

Fig. 2. Comparison of the human experimental blood:air partition coefficients with the QSPR-derived estimates. Regression of two subsets of VOCs are presented.

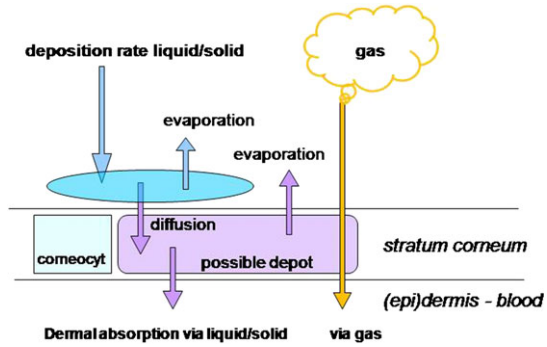

Fig. 3. Scheme of the absorption processes as modelled according to the Skinperm algorithm.

Table 2. Aggregation of tissues for tissue:blood partitioning

Tissue	Adopted tissue similarity in IndusChemFate model
Fat	Fat
Liver	Liver, intestine
Muscle	Muscle, bone, heart, lung, skin
Kidney	Kidney
Brain	Brain, bone marrow

$$\mathrm{PCtb} = \frac{0.133 \times K_{\mathrm{OW}}^{0.48} + 0.775}{0.0056 \times K_{\mathrm{OW}}^{0.48} + 0.830} - 0.21 \quad (5)$$

with PCtisbl = brain:blood partition coefficient; K_{ow} = octanol:water partition coefficient.

The octanol:water partition coefficients were taken at the physiological pH of 7.4. This considers the speciation of extent of ionization of the substance. These data were retrieved from databases of physical–chemical properties of chemicals [EPIsuite database of US-EPA (2009), the Chemspider database (RSC, 2010)].

Application of this equation to adipose tissue results into negative partition coefficients in case of $\log(K_{ow}) < 0.4$. This has no scientific meaning. So if the partition coefficient adipose tissue:blood is estimated to be <0.1, the adipose tissue:blood partition coefficient is fixed to 0.1.

Modelling of uptake of chemicals

Tissue concentrations for each of the chemicals and metabolites can be simulated for either acute,

occupational, or environmental exposure regimes with its typical duration, routes, concentrations, or dose rate. The impact of exercise that may influence uptake, distribution, metabolism, and excretion is accounted for by two levels of exercise (at rest and at light exercise, with a heart rate of, respectively, 78 and 114 beats min^{-1}) with corresponding physiology parameters (cardiac output and pulmonary ventilation) according to Gale *et al.* (1985). The increase of the cardiac output was mainly assigned to the muscle blood flow and the arterial liver blood flow and the lung blood flow was set the same fraction of the cardiac output as in rest. The blood flows through other compartments were set equal to that in rest.

Inhalation in the IndusChemFate PBTK model is controlled by the concentration of the compound in the inhaled air, the alveolar ventilation, and the blood:air partition coefficient. In the model, the maximum concentration in inhaled air is limited at the level of saturated vapour pressure. The actual concentration in inhaled air can be lower than the environmental air concentration due to wearing of respiratory protective equipment (= RPE). The reduction factor of the RPE can be entered. The default respiratory reduction factor 1 (= no RPE).

In the last two decades, the awareness has grown that dermal absorption of chemicals after environmental and/or occupational exposure can be very significant. This has lead to the development of PBPK models with an integrated dermal compartment (Corley *et al.*, 2000; Reddy *et al.*, 1998) as well as dermal only PBPK models (McCarley and Bunge, 1998; McCarley and Bunge, 2000; Kim *et al.*, 2006a,b; van der Merwe *et al.*, 2006; Kim *et al.*, 2007; Reddy *et al.*, 2007). These models typically require many (experimentally determined) input parameters. We applied a modified version of the algorithm as developed by ten Berge (2009) and Wilschut *et al.* (1995) in our PBTK model. This so-called Skinperm algorithm is a diffusion-based physiological model that predicts absorption based on physical–chemical properties of the substance. It distinguishes two pathways of permeation through the skin: trans-cellular and inter-cellular. The physiological model considers the following processes:

(1) Dermal deposition of a substance (liquid) on the skin,
(2) Diffusion to the stratum corneum (SC), and
(3) Absorption to the dermis/blood flow.

After or during deposition of a liquid or solid substance on the skin, evaporation of the substance and dermal absorption will start simultaneously (see scheme in Fig. 3). Depending on the balance of mass flows in the skin, a depot may be formed in the stratum corneum. This happens when a substance diffuses easily into the stratum corneum but is slowly absorbed by the dermis. Such a depot will cause continuation of the absorption also when the deposition on the skin has stopped. Critical parameters are the aqueous dermal permeation coefficient and the stratum corneum/water partition coefficient. Both parameters are estimated by means of QSPRs, developed by ten Berge (2009). For the estimation of the aqueous permeation coefficient, the $\log(K_{ow})$ is required. Since the pH of the stratum corneum is 5.5 the $\log(K_{ow})$ at this pH should be taken. It is known that the $\log(K_{ow})$ may vary at different pH, especially for organic acids and bases. The example of nicotine shows that this may affect the skin absorption dramatically (Zorin *et al.*, 1999).

The dermal absorption from the vapour phase is also considered (see Fig. 2). Direct transdermal uptake of vapour in the air might take place by diffusion. In order to model this, the aqueous permeation coefficient is transformed to a dermal air permeation coefficient as described by Wilschut *et al.* (1995), considering vapour pressure of the compound and resistance of a certain stagnant air layer direct on the skin. The isolation value of light clothing is considered to be equivalent to an assumed 3–10 cm stagnant air layer. Depending on the physical activity of the person, this layer is estimated to be 3 cm (= at light work) or 10 cm (= at rest) thick. Airtight clothing will reduce the vapour concentration available to skin absorption. The reduced uptake can be modelled with a dermal protection factor. The default value = 1 (no airtight clothing). However, when an airtight suit with a dermal protection factor of 10 is applied, the actual air concentration near the skin in the model is 10-fold decreased.

Oral intake of compounds is considered as a bolus dose that is applied to the intestinal lumen (via the stomach) and then absorbed into the intestinal tissue at a first order rate. From the intestines, the compound is released to the blood stream towards the liver (portal vein). The first order absorption rate is defined as the velocity at which the oral dose is absorbed by the intestinal tissue (as a fraction of the dose in the lumen per hour). Stomach and intestines are lumped in the model. The oral dose [in milligrams per kilogram body weight (BW)] and the absorption rate are the required input parameters for oral uptake in the model.

Enterohepatic circulation

Phase II metabolism with conjugation of metabolites generally increases the solubility. Enzymes produced by intestinal bacteria—such as β-glucuronidase, sulfatase, and various glycosidases—deconjugate these compounds in the intestines, releasing the parent compounds after which these are readily reabsorbed across the intestinal wall to the blood. This results in enterohepatic circulation (of conjugated phase II metabolites). Few published PBPK models consider enterohepatic circulation (Collins *et al.*, 1999; Teeguarden *et al.*, 2005). These models require experimental data for transfer rates. In our model, we applied a generic approach: it incorporates enterohepatic circulation by defining the ratio of excretion to bile relative to excretion to the blood. This ratio is defined as the fraction of the amount of a metabolite in liver tissue that is excreted to the intestinal lumen via bile. In this approach, bile excretion means that there is an intestinal reabsorption.

If, for example, the removal ratio of a non-conjugated metabolite from the liver by enterohepatic circulation is set 0, there is no enterohepatic circulation. If in the case of a conjugated metabolite, the removal ratio is set to 1, 50% of the total amount that leaves the liver per unit of time is excreted to blood, and 50% to the intestinal lumen via bile, available for reabsorption with a fixed rate of 0.3 h^{-1}.

Elimination

The chemical in the human body is eliminated in the model by two processes: metabolism (or biotransformation) and direct excretion in air or urine.

Biotransformation is described by Michaelis–Menten saturable metabolism following the mathematical algorithms as described by Ramsey and Andersen (1984). The (parent) compound is metabolized by a set of (iso)-enzymes. Usually, one or more metabolite(s) are produced. Metabolites may either undergo further metabolism or will be excreted.

Contrary to many PBPK models, the occurrence of metabolism is not limited to the liver compartment but can be considered in any of the 11 model compartments. However, the default setting is metabolism in the liver only. Metabolic kinetic parameters are the maximum velocity of metabolism [$= V_{max}$ in μmol/(kg tissue × h)] and the Michaelis–Menten constant ($=k_M$ in μM). Preferably, these values are taken form experimental data with human tissue. Conversion of reported experimental V_{max} to the proper units is given in the addendum.

When parallel metabolic pathways are involved, the V_{max} and k_M values for a specific metabolite production can be set as different from those the parent compound. That is possible because the model considers both removal of the parent compound and production of metabolite as separate steps. That means the biotransformation of the parent compound occurs for only x% into the metabolite of interest and for (100−x)% into other (unknown) metabolites. V_{max} and k_M metabolism constants of a series of VOC have recently been summarized (Aylward *et al.*, 2010).

Substances can be excreted via urine, either unchanged as parent compound or as a metabolite. DeWoskin and Thompson (2008) published a paper in which renal clearance is modelled in great detail; however, the required input data transcends application in a generic model. Urinary excretion is mainly based on the lipophilicity of substances, assuming that lipophilic substances are less water soluble and therefore excreted via urine to a lower extent. The QSPR as developed by DeJongh *et al.* (1997) that calculates the solubility in blood based on lipid fractions in blood is therefore adopted in the syntax of the model. It is assumed that human blood contains 0.7% lipids. See formula 6.

$$\mathrm{FrWsol} = \frac{0.993}{0.993 + 0.007 \times 10^{\log(K_{ow})}} \qquad (6)$$

with FrWsol = water soluble fraction in blood, $\log(K_{ow})$ = log(octanol:water partition coefficient).

The model takes into account the renal clearance of substances by means of ultrafiltration in the glomeruli and possible resorption to the blood in the tubuli. The total renal clearance is assessed as the glomerular filtration minus the resorption in the tubuli. The model assumes that 8% of arterial blood becomes primary urine. The glomular filtration rate in the IndusChemFate PBTK model is therefore set at 0.08 of the renal arterial blood flow. Tubular resorption restricts the renal clearance to 1% of the glomerular filtrate (Griffiths, 1974). The tubular resorption is either set on or off. The selection is based on the octanol–water partition coeffient ($\log(K_{ow})$) of the substance or metabolite of interest. The cut-off is arbitrarily set to a $\log(K_{ow})$ value of −1.5 measured at pH 7.4. This is close to the $\log(K_{ow})$ of water (−1.38). Water is fully resorbed by the kidney. Very soluble substances with a $\log(K_{ow}) < -1.5$ are assumed not to be resorbed. This approach is basic and will result in a relative inaccurate estimate when log (K_{ow}) is close to −1.5. This disadvantage is accepted in favour of simplicity of the approach.

The total volume of excreted urine in 24 h is set to 1.44 l.

When the volatility is high, chemicals (and in a few cases a metabolite) will be exhaled. The exhaled concentration is a mixture of the inhaled air concentration (air that has not reached the alveoli) and alveolar air. The concentration of a compound in the alveolar space of the lungs is controlled by the blood concentration in the (arterial) lung blood and the blood: air partition coefficient. The amount of a compound that is exhaled is calculated by multiplying the alveolar concentration by the alveolar ventilation rate.

Mass balance

After every model simulation, a mass balance is calculated. Absorbed amounts per route are summarized and compared with the total of excreted amounts, amounts in tissues, and amounts to undefined metabolites, not assigned to the metabolic route considered.

The Excel application of the PBTK model

The generic PBTK model is available as a spreadsheet application in MS Excel. The differential equations of the model are programmed in Visual Basic. The spreadsheet template can be operated after a few instructions. The numerical integration is fast. A typical simulation of 24 h after exposure takes a few seconds on a standard personal computer, including the plotting of the results.

The full mathematical description of the PBTK model is presented in Supplementary 1 (available at *Annals of Occupational Hygiene* online) in the online edition. The mathematical description of dermal absorption of chemicals is presented in supplement 2 in the online edition.

Output is presented as numerical listing over time in tabular form and in graphs. The program does provide the amounts in micromoles and concentrations in micromoles per litre. After each run, amounts and concentrations in compartments and fluids are listed together with the estimated partition coefficients of the chemical and metabolites under study and the data of the mass balance. Also, graphs of the concentrations in alveolar air, blood, and urine are presented.

The IndusChemFate PBTK model is available free of charge from the CEFIC-LRI website as a Visual Basic application in Microsoft Excel (available at http://www.cefic-lri.org/lri-toolbox/induschemfate last accessed on 7 September, 2011).

EXPERIMENTAL

Studies with exposure to chemicals (inhaled concentration or dermal dose rate) and with repeated measurements of concentration of the chemical and metabolites in blood and/or urine were searched for. Six experimental or observational studies with six different compounds were selected, e.g. the compounds pyrene (Jongeneelen *et al.*, 1988), methyl-tert-butylether = MTBE (Amberg *et al.*, 1999), *N*-methyl-pyrrolidone = NMP (Bader *et al.*, 2008), ethanol (Kramer e*t al.*, 2007), 2-butoxyethanol = 2-BE (Franks *et al.*, 2006), and n-heptane (Rossbach *et al.*, 2010). The occupational exposure scenarios of the studies were different.

The time course of the blood and urine concentrations of the parent compound and/or metabolites were simulated with the PBTK model IndusChemFate following the reported exposure scenario of the selected study. The physical—chemical input parameters of the compounds—molecular weight, density, vapour pressure, log(octanol:water) partition coefficient at pH 5.5 and at 7.4, and water solubility—were taken from the EPI suite database of US-EPA (2009), the Chemspider database (RSC, 2010). The results of the simulations (shape and height of the predicted concentrations) were compared with the reported experimental results. All simulations were done with PBTK model IndusChemFate, version 1.6.

RESULTS

Comparison 1: excretion of hydroxylated metabolite of pyrene in creosote impregnating worker

The concentration of a 1-hydroxypyrene (1-OHP, a hydroxylated metabolite of pyrene) was measured in urine of an operator of a creosote impregnating site (Jongeneelen *et al.*, 1988). Urine was collected twice a day over a period of 7 days, from Tuesday to Tuesday, in which 5 days were working days. 1-OHP was measured as the sum of free and conjugated 1-OHP. The concentration of 1-OHP in urine over the week is presented in Fig. 4. The concentrations were taken from the figure of the original paper. The increase of 1-OHP in urine over the week is obvious and some accumulation over the week is observed.

The excretion of 1-OHP was simulated with the PBTK model IndusChemFate. Reported exposure data of creosote plant operators of other studies were used to make an estimate of the representative exposure scenario. Airborne exposure of creosote plant operators to pyrene might be up to 3 μg m^{-3} (and is present as vapour, Borak *et al.*, 2002). It has been postulated that among creosote impregnating workers, the dermal route account for up to 90% of the body dose (van Rooij *et al.*, 1993; Elovaara *et al.*, 1995; Borak *et al.*, 2002). Dermal load rate

measurements of pyrene ranges from ND—90 ng cm^{-2} skin in 8-h work shift; the exposed dermal surface area is large: neck, wrist, and jaw/neck of creosoting workers were clearly exposed (van Rooij *et al.*, 1993). The average total exposed skin area of the creosote impregnating workers was estimated to be 7500 cm^2. Thus, a representative exposure scenario of creosote plant operator to pyrene is 8-h Time Weighted Average (TWA) exposure to 3 μg m^{-3} and dermal exposure of a skin surface of 7500 cm^2 to a skin loading rate of 45 ng cm^{-2} per 8-h shift = 6 ng × cm^{-2} × h^{-1}.

This exposure scenario was used to model the time course of the concentration of 1-OHP and 1-OHP-gluc in urine in the PBTK model IndusChemFate. It was assumed that half of the amount of the absorbed pyrene is metabolized to 1-OHP, followed by 100% glucuronidation of 1-OHP to 1-hydroxpyrene-glucuronide (= 1-OHP-gluc). That means that is assumed that the other half of the amount of pyrene is converted to unidentified metabolites.

The PBTK model requires input data of three compounds: the parent compound pyrene, 1-OHP, and 1-OHP-gluc. The physical–chemical input data and the kinetic input data are presented in Table 3.

The simulation showed that 1-OHP-gluc is the dominant metabolite in urine. Free 1-OHP was predicted to be is <0.1% of 1-OHP-gluc. The simulated excretion pattern of 1-OHP-gluc of the last 4 days of a working week is shown in Fig. 4. The level and shape of the simulated excretion pattern of 1-OH-pyrene-glucuronide are quite similar to the measured data of Σ (free + conjugated) 1-OH-pyrene. It is known that the majority of 1-OHP is excreted in urine as conjugated to glucuronide (Strickland *et al.*, 1994). After an enzymatic hydrolysis with glucuronidase, the level of free 1-OHP was 7-9 fold increased (Jongeneelen *et al.*, 1987a), suggesting that free 1-OHP is <15% of 1-OHP-gluc. The predicted pattern of urinary 1-OHP in a period of several days with 8-h occupational exposure shifts and a weekend off work is well comparable with the experimental findings. Additional simulations with single route inhalatory and dermal exposure confirmed that dermal uptake is an important exposure route. In the present scenario of exposure, dermal uptake accounted for 60% of the body burden.

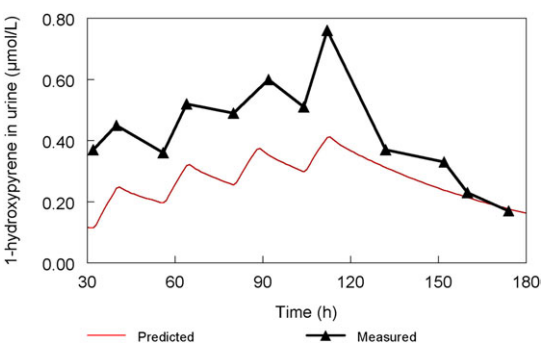

Fig. 4. Excretion of 1-OHP in urine of a creosote impregnating worker. Indicated is the measured excretion of total of free and conjugated 1-OHP in urine (converted to micromoles per litre units taken from Jongeneelen *et al.*, 1988) and the model predicted excretion of 1-OHP-gluc.

Comparison 2: blood and urine concentrations of MTBE and metabolites after inhalation

Six volunteers (three males and three females) were exposed to a concentration of 40 p.p.m. MTBE (methyl-tertiary-butylether) (= 144 mg m^{-3}) for 4 h in a dynamic exposure chamber (Amberg *et al.*, 1999). The airborne MTBE concentration was determined at 15-min interval. The measured level was 38.6 ± 3.2 p.p.m. = 140 mg m^{-3}. Urine of the volunteers was collected at given intervals over 72 h. Blood was sampled at the end of the exposure period.

Figure 5 shows the time course of urinary excretion of the two main metabolites

2-methyl-1,2-propanediol (MPD) and 2-hydroxyisobutyrate (HiBA) as reported by Amberg *et al.* (1999). HiBA was the predominant metabolite. Blood samples were tested for MTBE and t-butanol.

In the body, MTBE is metabolized to tert-butanol (Metabolite 1). This metabolite is further metabolized, mainly to MPD (Metabolite 2), which is further oxidized to HiBA (Metabolite 3).

The fate of MTBE and three metabolites in blood and urine was simulated with PBPK model IndusChemFate with the given scenario of exposure: 4-h exposure to a concentration of 140 mg m^{-3}. The entry data of MTBE and the three metabolites that were used for the simulation are presented in Table 4. Estimates for the kinetic constants of the conversion of MTBE to tert-butanol were derived from *in vitro* experiments with human liver preparation (Licata *et al.*, 2001). The kinetic constants of the subsequent metabolic steps were not found in the literature and were estimated set on the basis of expert knowledge. The model predicted a level of HiBA in urine that is close to the observed level. Amberg *et al.* (1999) reported also the total amount of MTBE and metabolites excreted in urine over 72 h. In Table 5, the reported amounts are presented together with the model-predicted amounts. The results show that the level of agreement is satisfactory, except for the metabolite MPD; this level is clearly

Table 3. Input data for the simulation of pyrene, 1-OHP. and 1-OHP-gluc in the PBTK model

Compound / *Property*	*Pyrene*	*1-OHP*[a]	*1-OHP-gluc*[b]
CAS reg. Nr.	129-00-0	5315-79-7	154717-05-2
Density (g/L)	1270	1000	1000
Molecular weight	202.26	218.28	394
Vapour Pressure (Pa)	0.0106	0.000022	3.2E-17
Log(K_{ow}) at skin pH 5.5	4.88		
Log(K_{ow}) at blood pH 7.4	4.88	4.45	-2.12
Water solubility (mg/L)	0.135	2.77	40,000
Resorption tubuli (y/n/?)	y	y	n
Enterohepatic removal (relative to liver venous blood)	0	0	0.3
V_{max} liver of removal (µmol/(kg tissue * h))	360 (Removal of pyrene, estimate)	6,900	
k_M liver of removal (µmol/L)	4.5 (Removal of pyrene, estimate)	7.7	
V_{max} liver of metabolite production (µmol/(kg tissue * h))	180[c] (Formation 1-OHP; Jongeneelen et al, 1987b)	6900[d] (Formation 1-OHP-gluc; Luukkanen et al, 2001)	
k_M liver of metabolite production (µmol/L)	4.5 (Formation 1-OHP; Jongeneelen et al, 1987b)	7.7 (Formation 1-OHP-gluc; Luukkanen et al, 2001)	

[a]1-OHP data from EPIsuite and/or chemspider.
[b]Log(K_{ow}) and water solubility is estimated by cross reading of values of similar glucuronides as *N*-Glucuronide of *N*-hydroxy-2-aminofluorene.
[c]V_{max}1-OHP = 0.18 × 1 000 000 = 180 000 nmol h^{-1} kg^{-1} liver tissue.
[d]It is assumed that the S9 corresponds with a protein content of 20 mg protein per ml liver (Chalbot *et al.*, 2005) which is assumed to correspond roughly with 20 mg g^{-1} liver. V_{max}1OHP-gluc = 5.8 × 20 000 (milligrams protein per kilogram liver) x× 60 (min) = 6 900 000 nmol h^{-1} kg^{-1} liver tissue.

underestimated. The reason for this difference may be an incomplete metabolic approach for the model. Amberg *et al.* (1999, 2001) listed tert-butanol as primary metabolite of MTBE, MPD as second metabolite, and HiBA as tertiary metabolite. Moreover, they mentioned the glucuronidation of tert-butanol as an important bypass reaction. However, glucuronidation or another conjugation of MPD

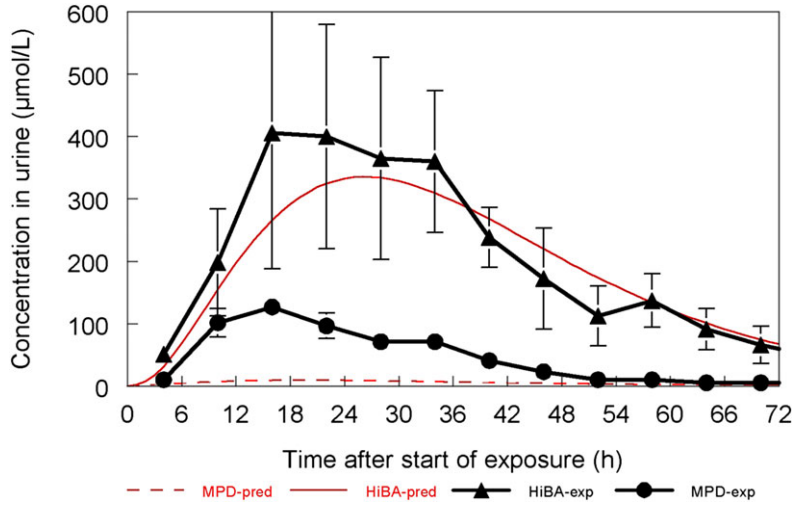

Fig. 5. Two metabolites of MTBE in urine after 4-h constant exposure to 140 mg m^{-3} MTBE at resting conditions. Experimental data are from Amberg *et al.* (1999). Exp, experimental; pred, model-predicted. MPD, methylpropanediol; HiBA, hydroxyisobutyrate.

may also happen. Because Amberg *et al.* (1999, 2001) quantified the urinary concentration of MPD after acidic hydrolysis, measuring both the sum of free and the conjugated MPD. In the model, the physical–chemical properties of non-conjugated MPD, e.g. water solubility of 238 g l^{-1}, were entered only. If a part of MPD occurs as conjugate, this will result in an increased urinary excretion of MPD and a lower excretion of HiBa.

Furthermore, blood levels were reported. The concentration of MTBE and t-butanol in blood was determined at the end of the 4-h exposure period. Table 6 shows the measured and predicted concentrations of MTBE and t-butanol in blood. The model-predicted concentration of MTBE and the metabolite t-butanol is in the same order of magnitude.

The mass balance showed that exhalation of MTBE was the preferred route of elimination; the exhaled amount of excreted MTBE and metabolites in 48 h was 2-3 fold larger than the excreted amount in urine (respectively, 34 µmol kg^{-1} BW and 13.2 µmol kg^{-1} BW).

Comparison 3: urine concentrations of NMP after transdermal vapour absorption

Dermal vapour phase absorption is an important route of uptake of the solvent *N*-methyl-2-pyrrolidone (NMP). This particular aspect was investigated in an experimental study with 16 volunteers exposed to 80 mg m^{-3} NMP for 8 h under either whole body, i.e. inhalation plus dermal vapour exposure, or dermal only conditions (Bader *et al.*, 2007; 2008). The scenario of dermal vapour exposure only was realized in experiments of exposed volunteers with face shield masks and supply of active carbon filtered air. The exposure period was 2 × 4 h with an exposure-free interval of 30 min. The urinary excretion of NMP and its main metabolites 5-hydroxy-*N*-methyl-2-pyrrolidone (5-HNMP) and 2-hydroxy-*N*-methylsuccinimide (2-HMSI) was measured. Exposure to a concentration of 80 mg m^{-3} NMP under resting conditions resulted in urinary peak concentrations of 20 µMol l^{-1} of NMP, 800 µMol l^{-1} of 5-HNMP, and 200 µMol l^{-1} of 2-HMSI (converted to micromoles per litre from the data of the original publication). The measured concentration of NMP and metabolites after exposure to 80 mg m^{-3} is presented as continuous lines in Fig. 6A,B. Bader *et al.* (2008) concluded that dermal absorption from the vapour phase contributes significantly to the total uptake. The levels suggest that ~50% of the body burden is derived from transdermal uptake of vapour.

The fate of NMP and metabolites after 8-h exposure to a concentration of 80 mg m^{-3} was simulated with PBPK model IndusChemFate. The chemical-specific data of NMP and metabolites that were used for the simulation are presented in Table 7. Ligocka *et al.* (2003) published data on the metabolism kinetics in human liver microsomes. 5H-NMP formation followed Michaelis–Menten kinetics with a V_{max} of 1.1 nmol min^{-1} mg^{-} protein and a k_M of 2.4 mM. For the simulation, we supposed that NMP has a single route of metabolism, from NMP → 5-HNMP → MSI → 2HMSI, with V_{max} and k_M for each step as shown in Table 8.

Table 4. Input data for the simulation of MTBE and its main metabolites in the PBTK model

Compound / *Property*	*MTBE*	*t-Butanol (= metabolite 1)*	*2-Methyl-1,2-propanediol (= metabolite 2)*	*2-Hydroxy-isobutyrate (= metabolite 3)*
CAS nr	1634-04-4	75-65-0	558-43-0	594-61-6
Density (g/L)	740	781	1000	1000
MW	88.15	74.12	90.12	104.11
Vapour pressure (Pascal)	33,300	5,430	30	0.01
Log(K_{ow}) at pH 5.5	0.94			
Log(K_{ow}) at pH 7.0	0.94	0.35	-0.33	-4.09
Water solubility (mg/L)	51,000	1,000,000	238,000	1,000,000
Resorption tubuli (y/n/?)	y	y	y	n
Enterohepatic removal (relative to venous blood)	0	0	0	0
V_{max} liver of removal (µmol/(kg tissue * h))	500	300	300	
k_M liver of removal (µmol/L)	50	50	100	
V_{max} liver of metabolite production (µmol/(kg tissue * h))	500	300	300	
k_M liver of metabolite production (µmol/L)	50	50	100	

Table 5. The excreted amount of MTBE and MTBE metabolites in urine after inhalation of 140 mg m^{-3} over 72 h

	Measured total excretion in 72 h (corrected for background) (in µmol)	PBTK model-predicted total excretion in 72 h (corrected for background) (in µmol)
MTBE	2.0	5.9
t-Butanol	29.3	10.8
2-methyl-1,2 propane-diol	205	22.4
2-hydroxyisobutyrate	722	887

The predicted excretion of NMP and its main metabolites 5-hydroxy-NMP and 2-hydroxy-MSI in urine is shown as discontinuous lines in Fig.ure 6A,6B. The simulation shows also that 50% in the body dose is derived from transdermal uptake of vapour. However, the simulation did not clearly show that transdermal uptake of the vapour did delay the elimination peak times of NMP and 5-HNMP.

In Table 10, the actual total urinary elimination of NMP and two main metabolites over 48 h after

Table 6. MTBE and t-Butanol in blood of volunteers after 4 h of inhalation

Substance	Measured by Amberg *et al.* (1999)		PBTK model Predicted
	After 4 h inhalation of 140 mg m^{-3} MTBE (in µmol l^{-1})	Background (in µmol l^{-})	After 4- h inhalation of 140 mg m^{-3} MTBE (in µmol l^{-1})
MTBE	6.7	n.d.	15.9
t-Butanol	21.8	0.9	7.37

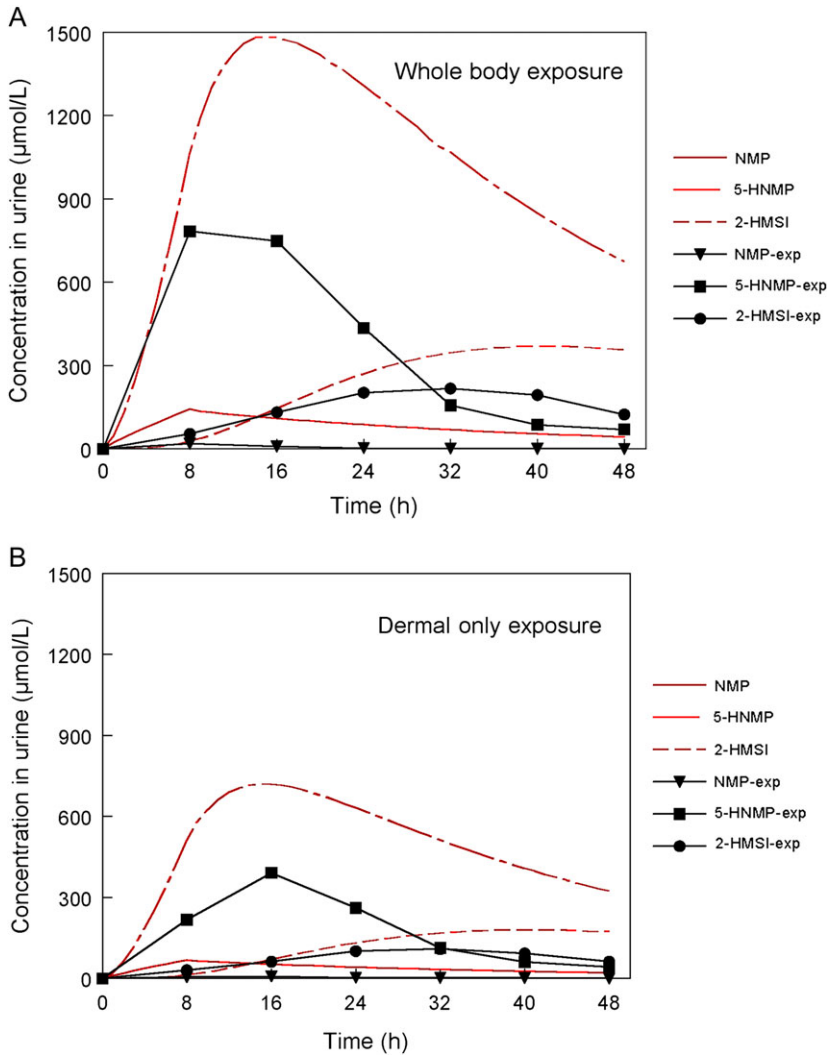

Fig. 6. Excretion of NMP and two metabolites in urine after 8-h exposure to 80 mg m^{-3} NMP. Two scenarios are presented: whole-body exposure (A) and dermal-only exposure using 100% respiratory protection (B). (NMP = *N*-methyl-2-pyrrolidone, 5-HNMP = metabolite 5-hydroxy-N-methyl-2-pyrrolidone, and 2-HMSI = metabolite-hydroxy-N-methylsuccinimide. Exp, experimental data of Bader *et al.* (2008) and pred = model predicted).

whole-body exposure and under resting conditions is presented. The predicted amounts as simulated with the PBPK model are also presented. The model overestimates the urinary elimination of NMP by 10-fold, but the predicted excreted levels of the two main metabolites are in the same range (2-3 fold difference).

Table 7. Input data of NMP and its main metabolites for the PBTK modelling

Compound / *Property*	*NMP*	*5-hydroxy-NMP (metabolite 1)*	*MSI (metabolite 2)*	*2-Hydroxy-MSI (metabolite 3)*
CAS nr	872-50-4	.	1121 -07-9	.
Density (g/L)	1030	1070	1000	1000
MW	99.12	115	113.12	129.12
Vapour pressure (Pascal)	46	1.10E-01	2.96E+00	6.86E-05
Log(K_{ow}) at pH 5.5	-0.38			
Log(K_{ow}) at pH 7.0	-0.38	-1.645	-0.95	-2.18
Water solubility (mg/L)	1,000,000	1,000,000	690,000	1,000,000
Resorption tubuli (y/n/?)	?	?	?	?
Enterohepatic removal (relative to venous blood)	0	0	0	0
V_{max} liver of removal (µmol/(kg tissue * h))	3,300	3,300	3,300	
k_M liver of removal (µmol/L)	2,400	1,200	1,200	
V_{max} liver of metabolite production (µmol/(kg tissue * h))	3,300	3,300	3,300	
k_M liver of metabolite production (µmol/L)	2,400	1,200	1,200	

Comparison 4—comparison measured versus modelled: experimental hand rubbing study of ethanol

A human experimental study was carried out with volunteers to examine the ethanol absorption that occurs during hand disinfection using alcohol-based hand rubs (Kramer *et al.*, 2007). Twelve volunteers applied hand rubs containing 85% ethanol (hand rub B). To mimic surgical hand disinfection, 20 ml of 85% ethanol solution was applied to hands and arms up to the level of the elbow 10 times for 3 min, with a break of 5 min between applications. The dermal exposure scenario lasted 80 min. The hand rub experiment was done in a room sized 37 m^3 with two open windows and an open door. No controlled air exchange occurred during applications. Between applications of hand rubs, volunteers were placed in a second room in which the use of alcohol-based hand rubs was not permitted (Kramer *et al.*, 2007).

Whole-blood samples were taken before and seven times after exposure (at 85, 90, 100, 110, 140, and 170 min after the start of the experiment). Blood concentrations of ethanol were determined

Table 8. Total urinary elimination of NMP and its main metabolites in 48 h after whole-body exposure and under resting conditions

Exposure scenario	Measured excretion in µmol (from Bader *et al.*, 2008) (mean ± SE)			Predicted excretion in µmol (generic PBPK model)		
	NMP	5-HNMP	2-HMSI	NMP	5-HNMP	2-HMSI
2 × 4 h–80 mg m^{-3}	25 ± 2	1072 ± 118	555 ± 40	251	3170	733

using headspace gas chromatography. The black markers in Fig. 7 show the average of the measured concentration of ethanol in blood of the volunteers at the reported time.

The time course of ethanol level in blood was predicted with the PBTK model IndusChemFate. The volunteers were assumed to have light exercises. The metabolic rate constants V_{max} and k_M of the first step in the metabolism of ethanol are taken from Umulis *et al.* (2005). The entry values are shown in Table 9, together with the required chemical-specific data.

The exposure period lasted 80 min. In that period, 20 ml (= 16.5 g) of disinfectant fluid was 10 times applied on an estimated skin area of 2000 cm^2. The dose rate was estimated as (16.5 × 85%/100% × 10 × 60 min/80 min)/2000 cm^2 = 52.5 mg/(cm^2 × h). The solid line of Fig. 6 shows the predicted time course of ethanol in blood.

However, the ethanol solution on the skin will partly evaporate, thus inhalation of ethanol will also have contributed to the total uptake of the volunteers. Unfortunately, the inhalation exposure during the experiment was not recorded. Based on the ethanol mass emission rate during the experiment [(16.5 × 10)/80 = 2.063 g min^{-1}], an estimated room supply rate of 3 m^3 min^{-1} and the known volume of the room of experiments [37 m^3], the TWA concentration in the air of the room of the experiments was estimated using the well-mixed room model of IH-Mod (AIHA, 2010) as 580 mg m^{-3}. The volunteers remained in a second room between the applications of hand rubs. In the second room, the use of alcohol-based hand rubs was not permitted. The blood samples were immediately collected after the experiment in a third room. That all means that the TWA exposure of the volunteers over the experimental period of 80 min was estimated to be the half of the concentration in the first room = 290 mg m^{-3}.

This scenario of dermal exposure plus additional inhalation of 290 mg m^{-3} was used in a second simulation of the time course of ethanol in blood. It is

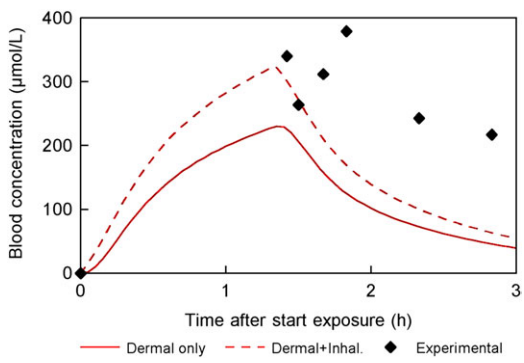

Fig. 7. Ethanol in blood after 10 times hand rubbing in a period of 80 min with a disinfection fluid containing 85% ethanol. Experimental data are from Kramer *et al.* (2007). Predicted is the concentration after dermal-only uptake and after dermal uptake + inhalation.

Table 9. Input data of ethanol for the PBTK modeling

Compound / *Property*	*ethanol*
CAS nr	64-17-5
Density (g/L)	789
MW	46.07
Vapour pressure (Pascal)	7,910
Log(K_{ow}) at pH 5.5	-0.31
Log(K_{ow}) at pH 7.0	-0.31
Water solubility (mg/L)	789,000
Resorption tubuli (y/n/?)	y
Enterohepatic removal (relative to venous blood)	0
V_{max} liver of removal (µmol/(kg tissue * h))	132,000
k_M liver of removal (µmol/L)	1,000
V_{max} liver of metabolite production (µmol/(kg tissue * h))	132,000
k_M liver of metabolite production (µmol/L)	1,000

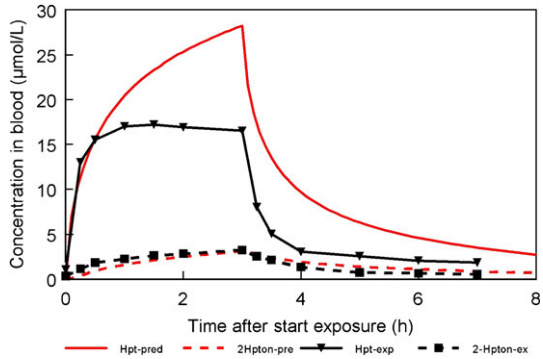

Fig. 8. n-Heptane(=hpt) and 2-heptanone (=hpton) in blood after 3-h constant exposure to 2000 mg m^{-3} heptane at resting conditions. Experimental data (=exp) are from Rossbach *et al.* (2010). The model-predicted concentrations of n-heptane and 2-hpton are also presented.

indicated as the broken line in Fig. 7. Compared to the ethanol blood level of dermal only scenario, the level is 20–30% higher.

Comparison 5: experimental inhalation study of n-heptane

A human experimental study was carried out with 20 male volunteers to examine the concentration profile of n-heptane, heptanols, and heptanones after exposure to the solvent in an exposure chamber (Rossbach *et al.*, 2010). The n-heptane concentration was 500 p.p.m. = 2000 mg m^{-3} for 180 min. Whole-blood samples were taken before, six times during exposure, and seven times after exposure (last at 1440 min = 24 h). Blood samples were analysed for n-heptane and seven of its mono-oxygenated metabolites with a new headspace solid phase concentration technique and GC–MS (Rossbach *et al.*, 2010).

The parent compound and its metabolites 2-heptanol and 2-heptanone were found in blood samples, with a decreasing level. The lines with marks in Fig. 8 shows the actual concentrations of n-heptane and 2-heptanone in blood of this scenario of exposure.

Table 10. Input data of n-heptane and two main metabolites for PBTK modelling

Compound / *Property*	*n-heptane*	*2-heptanol (metabolite 1)*	*2-heptanone (metabolite 2)*
CAS nr	142-82-5	543-49-7	110-43-0
Density (g/L)	695	818	808
MW	100	116	114
Vapour pressure (Pascal)	6,130	164	515
Log(K_{ow}) at pH 5.5	4.7		
Log(K_{ow}) at pH 7.0	4.7	2.31	1.97
Water solubility (mg/L)	3.4	3,270	4,300
Resorption tubuli (y/n/?)	y	y	?
Enterohepatic removal (relative to venous blood)	0	0	0
V_{max} liver of removal (µmol/(kg tissue * h))	14,000	18,000	14,000
k_M liver of removal (µmol/L)	1,100	80	1,100
V_{max} liver of metabolite production (µmol/(kg tissue * h))	14,000	14,000	
k_M liver of metabolite production (µmol/L)	1,100	500	

Table 11. Measured and estimated partition coefficients of n-heptane

Partition	Measured value (Perbellini *et al*., 1995)	Estimate of the PBTK model
Blood:air	1.9	3.65
Liver:blood	5.7	8.2
Kidney:blood	4.7	7.2
Brain:blood	6.5	13.2
Lung:blood	1.3	5.2
Heart:blood	3.2	5.2
Muscle:blood	6.6	5.2
Adipose:blood	202.6	142

The blood levels of n-heptane and 2-heptanone were predicted with the PBTK model IndusChem-Fate. Major metabolites of n-heptane are 2-heptanol and 2-heptanone, but the full scheme of the human metabolism is not known yet (Bahima *et al.*, 1984; Perbellini *et al.*, 1986; Szutowski and Rakoto, 2009). In the simulation, we supposed that n-heptane is metabolized to 2-heptanol. This metabolite is rapidly conjugated to the glucuronide and to 2-heptanone. Thus the metabolic conversion of the model is:

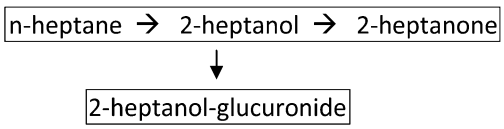

The kinetic metabolism constants of the successive steps of the metabolism of heptane are lacking. Thus, the kinetic metabolism parameters V_{max} and k_M were derived from the values of hexane (Hamelin et al, 2005). The metabolic clearance of 2-heptanol is high due to the conjugation of glucuronic acid, which is treated in the model as an undefined metabolite. The final values of n-heptane and two metabolites are shown in Table 10, together with the chemical-specific data.

Other routes to undefined metabolites were accounted for (metabolic clearance rate of removal of n-heptanol = 10 times the metabolic clearance rate of production of 2-hepatone). Thus, undefined metabolites are part of the model. The model-predicted concentrations in blood are represented in Fig. 8. The experimental and simulated concentrations of heptane and 2-heptanone in blood are within a range of 2 of each other.

n-Heptane is distributed among tissues, governed by tissue:blood partition coefficients, and the tissue-specific (arterial) blood flows. Perbellini *et al.* (1985) published data on the partitioning of industrial (C5–C7) solvents, including n-heptane, in human blood and tissues.

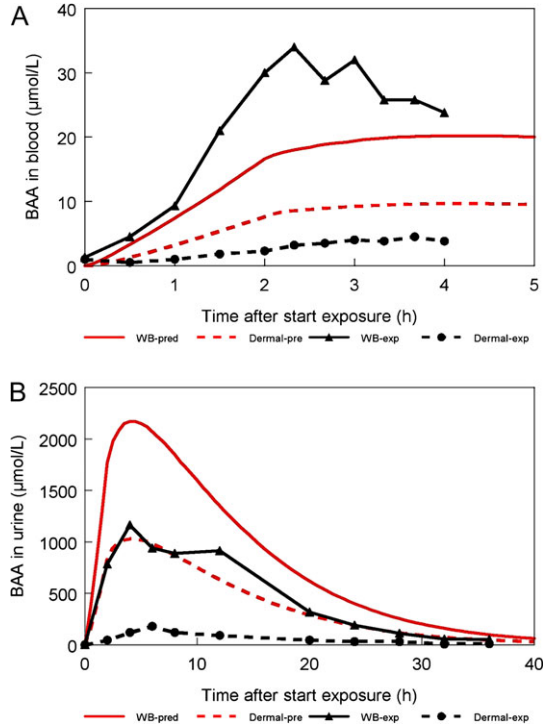

Fig. 9. Concentration of 2-butoxyacetic acid in blood (A) and in urine (B) after 2-h constant exposure to 256 mg m^{-3} 2-butoxyethanol at resting conditions (experimental data taken from Franks *et al.*, 2006). The whole-body exposure scenario (WB) and the dermal-only scenario (dermal) are presented.

Their data are based on blood:air and tissue:air partition in samples from two young men. The experimentally measured tissue:air coefficient was divided by the blood:air partition coefficient to get the tissue:blood partition coefficient. Table 11 shows the results.

In the PBTK model, the partitioning coefficient of tissue:blood for n-heptane is estimated. The QSPR predicted partition coefficients are also listed in Table 11. The predicted values were generally within 2-fold of the experimental values with the exception of the lung:blood partition coefficient.

Comparison 6: inhalation and dermal vapour uptake of 2-butoxyethanol

Inhalation and/or transdermal vapour uptake of 2-butoxyethanol (2-BE) has been studies in a series of human volunteer studies, for example, Johanson (1986), Johanson and Boman (1991), Corley *et al.* (1994, 1997), and Jones and Cocker (2003). Typical exposures range from 20 to 50 p.p.m. for 2–4 h at

Table 12. Input data of 2-butoxyethanol and metabolite 2 Butoxyacetic acid for the PBTK modelling

Compound / *Property*	*2-butoxyethanol*	*2-butoxyacetic acid (metabolite 1)*
CAS nr	111-76-2	2516-93-0
Density (g/L)	901.5	1,027
MW	118.18	132.16
Vapour pressure (Pascal)	117	0.1
Log(K_{ow}) at pH 5.5	0.86	
Log(K_{ow}) at pH 7.0	0.86	-2.87
Water solubility (mg/L)	901,000	1,000,000
Resorption tubuli (y/n/?)	y	?
Enterohepatic removal (relative to venouis blood)	0	0
V_{max} liver of removal (µmol/(kg tissue * h))	5,680	
k_M liver of removal (µmol/L)	200	
V_{max} liver of metabolite prodution (µmol/(kg tissue * h))	2,840	
k_M liver of metabolite production (µmol/L)	200	

rest or during light exercise (Jones and Cocker, 2003).

Jones and Cocker (2003) evaluated 2-butoxyacetic acid (BAA) as a biological marker in an experiment with exposure. Four volunteers were exposed to 50 p.p.m. (= 246 mg m^{-3}) 2-butoxyethanol vapour for 2 h via the whole-body exposure scenario and dermal-only scenario, taking samples at regular intervals. Dermal-only was a scenario in which the volunteers wore purified air supply respirators. The volunteers wore shorts with a T-shirt in both scenarios. Concentrations of BAA in the blood, free BAA in the urine, and total BAA in the urine were measured at regular intervals to determine the body burden during and after exposure to 2-BE. Franks *et al.* (2006) published the individual and average blood and urine levels of total BAA in blood (black lines in Fig. 8A) and urine (black lines in Fig. 9B). They showed that the transdermal uptake of 2-BE accounts for 16% to the total body burden.

The urine levels of 2-BE and BAA of this latter experiment were predicted with the PBTK model IndusChemFate. In man, 2-butoxyethanol is metabolized primarily via alcohol and aldehyde dehydrogenases, to butoxyacetic acid, the principal metabolite. 2-BAA is conjugated to glycine and other amino

acids. This is the favoured metabolic pathway for lower systemic doses of 2-butoxyethanol. Alternative pathways include O-dealkylation to ethylene glycol and conjugation to 2-butoxyethanol glucuronide and/or 2-butoxyethanol sulfate (Medinsky *et al.*, 1990).

In the PBTK model simulation, we used a metabolic conversion of 2-BE as:

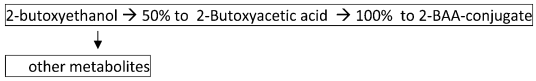

The metabolic kinetic constants V_{max} and k_M of the metabolism of 2-BE to BAA were taken from Johanson (1986) [respectively 5680 (μmol/(kg tissue × h and 200 μM)]. It is assumed that half of 2-BE is metabolized to BAA, the rest to undefined metabolites. The kinetic constants of the amino acid conjugation of 2-BAA were lacking and this route was not taken up in the model. The final metabolism constants of the compound and metabolite are presented in Table 12, together with the physical–chemical data.

The predicted concentration of 2-BAA in blood is presented in Fig. 9A, both after whole-body exposure and after dermal-only exposure. The blood concentrations are in the range of the measured values; however, inhalation seems underestimated and dermal uptake seems overestimated.

The predicted concentration of 2-BAA in urine is presented in Fig. 9B. Again, the predicted urinary concentrations are in the same range, but inhalation seems underestimated and dermal uptake seems overestimated.

Blood:air partition of 2-BE is high [a value of 7965 is reported by Johanson (1986), our model predicted a value of 7040]. Johanson introduced a correction factor for the alveolar uptake of 0.6 because of a washin–washout effect of polar highly water-soluble compounds during respiration. This correction was not adapted in our simulations.

DISCUSSION

The simulations of experimental results show that it is feasible to apply the PBTK model IndusChemFate to multiple chemicals, including metabolites and different exposure regimes. The simulations show that blood and urine concentrations of various chemicals can be predicted, given an exposure scenario with certain airborne concentration and/or a dermal deposition dose rate. The performance of the PBTK model IndusChemFate has been explored with the substances pyrene, MTBE, NMP, n-heptane, 2-butoxyethanol, and ethanol. The testing of the performance of the PBTK model has been focused on the parent compound and metabolites in blood and urine. The pattern of excretion of hydroxylated pyrene metabolites in a period of occupational exposure and off work could be predicted. The simulation of MTBE and metabolites in blood and urine is acceptable, but the results are not accurate in case of metabolite 2-methyl-1,2-propanediol. It might be that the uncertainty in the estimated metabolic rate constants hampers the accurate simulation of metabolites. In the case of NMP, it seems that the model overestimate the urinary elimination of NMP, but the predicted excreted levels of the two main metabolites are in the same order of magnitude. The comparison of experimental measurements of ethanol uptake showed that the fit of the experimental results with the predicted results of ethanol in blood are acceptable. The predicted blood values of n-heptane and 2-heptanone were generally within 2-fold. For 2-butoxyethanol, the predicted urinary concentrations are in the same range, but inhalation seems underestimated and dermal uptake seems overestimated. These comparisons illustrate that the estimated outcomes of simulations with different chemicals are within an order of magnitude.

Spaan *et al.* (2010) studied the interindividual variability of concentrations of biomarkers. They used results of 41 human volunteer studies that reported data of biomarkers of exposure. Volunteer studies were regarded as particularly useful as the volunteers received the same dose. The interindividual variation of the body fluid concentration of exposed volunteers in homogeneous groups expressed as GSD was 1.4 in average with an interquartile range of 1.21–1.75 and a range between the 5- and the 95-percentile of 1.1–2.4. Regarding the case of variation with a GSD of 2.4, the range between the boundaries expressed as the 5- and 95-percentile of the distribution, the interindividual difference is as large as ∼18-fold. This is the quantitative estimate of the boundaries of interindividual differences in exposed humans caused by various toxicokinetic processes. It seems that the interindividual differences can be very significant. Regarding the width of the interindividual differences of body fluid concentrations, it seems acceptable that the accuracy of this PBTK model of approximately an order of magnitude is acceptable for first tier predictions of body fluid concentrations of chemicals.

For testing, the usefulness of the PBTK model IndusChemFate, the V_{max} and k_M should come preferably from *in vitro* data and not from a PBPK model

optimization. Metabolic rate should at preference be derived in experiments measurements with microsomal liver fractions or with isolated hepatocytes. However, such *in vitro* measurements of the metabolic rate are not always available. Therefore, optimized V_{max} and k_M values from fitting procedures were used as a second best estimate. It should be pointed out that the use of such optimized parameters from earlier published chemical-specific PBTK models means only a check on the correctness of the algorithms of our PKTK model.

The biotransformation process can be modelled for subsequent metabolites. It has to keep in mind that many biotransformation steps may occur simultaneously. Therefore, we included the option of a different (higher) elimination and (lower) formation rate between transformed and created metabolite with specific Michaelis–Menten kinetics for each reaction. The kinetic constants describing saturable metabolism (V_{max} and k_M) in humans are essential data. These data can be found in studies of in vitro metabolism enzyme kinetics or in reviews, such as Aylward *et al.* (2010), who presented data of human metabolism kinetics of 51 VOCs. The apparent V_{max} and k_M measures provide in most cases a good match for the measured blood levels, but sometimes, these fitted rates fail to match the measured levels of metabolites in an accurate way. For example, Jones and Cocker (2003) showed in their of study of biological monitoring methods for 2-butoxyethanol that the ratio of free versus conjugated 2-BAA varies strongly between individuals. Such interindividual variation may interfere significantly, especially when the experimental group is little. The comparison of model-predicted with published experimental concentrations showed that when the value of crucial kinetic constants is not known, the results may become less accurate.

Partition coefficients of blood:air and blood:tissue are critical properties of the parent compound and metabolites, which control the distribution in the body next to blood flow and next to alveolar ventilation. The blood:air coefficients were estimated by a newly developed QSPR, making use of the 107 compiled experimental blood:air coefficients in humans of Meulenberg and Vijverberg (2000). These authors developed a QSPR algorithm for prediction of the blood:air coefficients with the independent variables saline:air and oil:air partition ratios. The octanol:air partition coefficient might be considered as a surrogate for the oil:air partition coefficient. So it was assumed that the blood:air partition coefficient is similarly related to the dimensionless Henry coefficient and the octanol:air partition coefficient of a substance. This assumption appeared to be valid. The regression coefficients of the independent variables, used in the QSPR, appeared to be highly significant. In the group of compounds with human partition data, the volatile substances appeared to be overrepresented. A separate algorithm for this subgroup of volatiles produced a better fit with measured values. Peyret *et al.* (2010) have recently published on a new model for estimating the tissue:blood partition coefficients. These authors take into account:

- Four matrices: tissue cells, tissue interstitial fluid, erythrocytes, and plasma.
- Matrix components: proteins, neutral lipids and acidic phospholipids, and water.
- Speciation of the substance at physiological pH or the extent of ionization.
- Partitioning on the basis of oil/water ratio, extent of ionization, and protein binding.

The authors elaborated their approach for adipose tissue, liver, and muscle. They showed the perfect similarity with earlier estimates from this science group with simpler models, but comparison with measured data was not shown. For our PBTK model, we were seeking for a simple approach. That is why we preferred to use the QSPR of DeJongh *et al.* (1997). They used an algorithm based on partitioning between blood and tissue on the basis of the water and lipid content of the two matrices: tissue and blood and the octanol:water partition coefficient. By using the octanol:water partition coefficients occurring at the physiological pH of 7.4, the speciation of extent of ionization of the substance is considered. We realize that this approach is less sophisticated than the more complex model of Peyret *et al.* (2010), but using the complex model would trigger a lot of effort for retrieving substance properties, which are not easily available.

An important feature of the present model is the prediction of transdermal absorption. Dermal absorption may take place after deposition of a liquid or solid compound on the skin and subsequent absorption from the contaminated skin area. Occupational exposure to vapour results into dermal absorption over the full body area. The QSPRs, developed by ten Berge (2009) for the aqueous permeation coefficient and the stratum corneum/water partition ratio play a pivotal role in the dermal absorption estimation by splash liquid contact and by vapour contact. Moreover, solvent evaporation during skin contact is fully accounted for and related to the volatility of the solvent. This has resulted in a novel approach of dermal uptake. The dermal

absorption of the solid pyrene and the liquid ethanol and of the vapours of the liquids *N*-methyl-pyrrolidone and 2-butoxyethanol was predicted within a factor of 2 of actually observed values for all these substances. It seems that the dermal module of the IndusChemFate model can contribute to a more accurate prediction of transdermal absorption of substances in cases of dermal exposure to chemicals.

Simulations with the PBTK model IndusChemFate result in single point estimates per unit of time. Neither bandwidth nor distribution with upper and lower confidence intervals is presented. The model is aimed to predict within one order of magnitude, corresponding to the average range of interindividual differences. Variability of output is not automatically presented since input of variables as distributions is not used. Nevertheless, the model calculates quick enough to run a high-low range of relevant parameters to get some feeling of the impact of parameter variability. Because a run usually does not require more than a minute, the influence of change of parameters can be explored in a couple of minutes.

For some chemicals, specific PBPK models has been published [.g. NMP (Poet *et al.*, 2010) and MTBE (Kim *et al.*, 2007; Leavens and Borghoff, 2009). These models vary in structure. It is acknowledged that chemical-specific PBPK models will provide more accurate predictions because of their extensive calibration to a particular chemical, but a general model for multiple chemicals has the advantage of being applicable to a wide variety of chemicals. This general applicability of the model is useful for screening studies where detailed data on partitioning are not available. An advantage of the current IndusChemFate PBTK model is that it can be consistently applied to different chemicals. A generic model allows multiple chemicals to be compared under standardized conditions, which could contribute to improved comparisons of the toxicokinetics of chemicals. The present PBTK model IndusChemFate can be regarded as first tier screening of fate of new and data-poor substances in human body.

The comparison with experimental studies shows that this PBTK model can help to explore and interpret results of human biomonitoring. The use of it may increase understanding of biomonitoring results. Also, a route-specific estimate may lead to a better understanding of contribution of each exposure route to total internal dose. The model could suggest a first tier estimation of biological equivalent guidance values (BEGV), based on external exposure limit of the substance.

The model described here, like all models, has limitations. It is designed primarily for neutral and predominantly ionic organic compounds, so inorganic kations that bind to specific tissues like bone tissue cannot be modelled because of their unusual partitioning properties. Currently, it is assumed that typical occupational and/or environmental exposures are too low to cause enzyme induction, which may result in a conservative overestimate of tissue concentration by underestimating degradation rates. Finally, the current model assumes that the physiological parameters of the person do not change by gender or over time, but gender and time differences are well known. Another limitation of the current model is its simplicity. The model lacks detailed descriptions for specific protein binding, intestinal transport, interaction with intestinal flora, and excretion by faeces that are important only for certain classes of chemicals. However, inclusion of detailed process descriptions increases the data demands for model applications. A simple model may also be sufficient for assessing the relative importance of the different elimination processes (urinary, respiratory, and metabolic elimination).

In summary, we have demonstrated that the developed PBPK model can be applied to multiple compounds with a degree of accuracy that can be regarded as a screening tool or as a first tier assessment. Such a first level model can exploit the results of environmental and occupational monitoring and modelling programs to deduce the routes of uptake, tissue concentrations, and body burdens. This PBPK model can contribute to an improved assessment of uptake of environmental and occupational contaminants.

In conclusion, the PBTK model IndusChemFate is a model for first tier or screening purposes, suitable in cases when only little is known of the toxicokinetics of a compound. One should realize that outcomes of the model should be interpreted within an accuracy of an order of magnitude. Especially when the quality of input data is limited the model outcomes become more uncertain.

Addendum

V_{max} is entered as μmol/(kg tissue × h). V_{max} is often expressed in per milligram microsomal protein. Conversion of the value of V_{max} expressed in per milligram microsomal protein or per number of hepatocytes is done using a recovery of 45 mg microsomal protein per gram liver or a recovery of 135×10^8 hepatocytes per gram liver (Blaauboer *et al.*, 1996). The liver weight of a 70 kg human being is 1.75 kg.

FUNDING

Long Range Initiative of CEFIC under contract nr. LRI-HBM2-ITC-0172.

SUPPLEMENTARY DATA

Supplementary data can be found at http://annhyg.oxfordjournals.org/.

REFERENCES

AIHA. (2010) Exposure Assessment Strategies Committee. IHMOD spreadsheet, January 2010. Available at http://www.aiha.org/insideaiha/volunteergroups/Documents/EASIHMOD%20HELP.pdf. Accessed 6 September 2011.

Amberg A, Rosner E, Dekant W. (1999) Biotransformation and kinetics of excretion of methyl-tert-butyl ether in rats and humans. Toxicol Sci; 51: 1–8.

Amberg A, Rosner E, Dekant W. (2001) Toxicokinetics of methyl tert-butyl ether and its metabolites in humans after oral exposure. Toxicol Sci; 61: 62–7.

Bader M, Wrbitzky R, Blaszkewicz M *et al*. (2008) Human volunteer study on the inhalational and dermal absorption of N-methyl-2-pyrrolidone (NMP) from the vapour phase. Arch Toxicol; 82: 13–20.

Bader M, Wrbitzky R, Blaszkewicz M *et al*. (2007) Human experimental exposure study on the uptake and urinary elimination of N-methyl-2-pyrrolidone (NMP)during simulated workplace conditions. Arch Toxicol; 81: 335–46.

Bahima J, Cert A, Menéndez-Gallego M. (1984) Identification of volatile metabolites of inhaled n-heptane in rat urine. Toxicol Appl Pharmacol; 76: 473–82.

Beliveau M, Krishnan K. (2005) A spreadsheet program for modeling quantitative structure-pharmacokinetic relationships for inhaled volatile organics in humans. SAR QSAR Environ Res; 16: 63–77.

Beliveau M, Lipscomb J, Tardif R, Krishnan K. (2005) Quantitative structure-property relationships for interspecies extrapolation of the inhalation pharmacokinetics of organic chemicals. Chem Res Toxicol; 18: 475–85.

Blaauboer BJ, Bayliss MK, Castell JV *et al*. (1996) The use of biokinetics and in vitro methods in toxicological risk evaluation. ALTA; 24: 473–97.

Borak J, Sirianni G, Cohen H *et al*. (2002) Biological versus ambient exposure monitoring of creosote facility workers. Occup Environ Med; 44: 310–19.

Brightman FA, Leahy DE, Searle GE, Thomas S. (2006) Application of a generic physiologically based pharmacokinetic model to the estimation of xenobiotic levels in human plasma. Drug Metab Dispos; 34: 94–101.

Cahill TM, Cousins I, Mackay D. (2003) Development and application of a generalized physiologically based pharmacokinetic model for multiple environmental contaminants. Environ Toxicol Chem; 22: 26–34.

Clewell HJ, III, Gentry PR, Covington TR, Gearhart JM. (2000) Development of a physiologically based pharmacokinetic model of trichloroethylene and its metabolites for use in risk assessment. Environ Health Perspect; 108 (Suppl. 2): 283–305.

Clewell HJ *et al*. (2001) Comparison of cancer risk estimates for vinyl chloride using animal and human data with a PBPK model. Sci Total Environ; 274: 37–66.

Collins AS, Sumner SC, Borghoff SJ, Medinsky MA. (1999) A physiological model for tert-amyl methyl ether and tert-amyl alcohol: hypothesis testing of model structures. Toxicol Sci; 49: 15–28.

Corley RA, Bormett GA, Ghanayem BI. (1994) Physiologically-based pharmacokinetics of 2-butoxyethanol and its major metabolite, 2-butoxyacetic acid, in rats and humans. Toxicol Appl Pharmacol; 129: 61–79.

Corley RA, Gordon SM, Wallace LA. (2000) Physiologically based pharmacokinetic modeling of the temperature-dependent dermal absorption of chloroform by humans following bath water exposures. Toxicol Sci; 53: 13–23.

Corley RA, Markham DA, Banks C *et al*. (1997) Physiologically-based pharmacokinetics and the dermal absorption of 2-butoxyethanol vapour by humans. Fundam Appl Toxicol; 39: 120–30.

DeJongh J, Verhaar HJ, Hermens JL. (1997) A quantitative property-property relationship (QPPR) approach to estimate in vitro tissue-blood partition coefficients of organic chemicals in rats and humans. Arch Toxicol; 72: 17–25.

DeWoskin RS, Thompson CM. (2008) Renal clearance parameters for PBPK model analysis of early lifestage differences in the disposition of environmental toxicants. Regul Toxicol Pharmacol; 51: 66–86.

ECHA. (2008a) Guidance on information requirements and chemical safety assessment Chapter R.7c—endpoint specific guidance. Appendix R.7.12-1 Toxicokinetics—Physiological Factors. Available at http://guidance.echa.europa.eu. Accessed 7 September 2011.

ECHA. (2008b) Guidance on information requirements and chemical safety assessment Chapter R8. Characterisation of dose [concentration]—response for human health. Appendix 8–4. Available at http://guidance.echa.europa.eu.

Elovaara E, Heikkilä P, Pyy L *et al*. (1995) Significance of dermal and respiratory uptake in creosote workers: exposure to polycyclic aromatic hydrocarbons and urinary excretion of 1-hydroxypyrene. Occup Environ Med; 52: 196–203.

Franks SJ, Spendiff MK, Cocker J *et al*. (2006) Physiologically based pharmacokinetic modelling of human exposure to 2-butoxyethanol. Toxicol Lett; 162: 164–73.

Gale GE, Torre-Bueno JR, Moon RE *et al*. (1985) Ventilation-perfusion inequality in normal humans during exercise at sea level and simulated altitude. J Appl Physiol; 58: 978–88.

Griffiths M. (1974) Introduction to human physiology In Chapter 27: The function of the kidney. New York: MacMillan Publishing Co. ISBN 0-02-347220-0.

Haddad S, Pelekis M, Krishnan K. (1996) A methodology for solving physiologically based pharmacokinetic models without the use of simulation softwares. Toxicol Lett; 85: 113–26.

Haddad S *et al*. (1999) Physiological modeling of the toxicokinetic interactions in a quaternary mixture of aromatic hydrocarbons. Toxicol Appl Pharmacol; 161: 249–57.

Haddad S, Charest-Tardif G, Tardif R, Krishnan K. (2000) Validation of a physiological modeling framework for simulating the toxicokinetics of chemicals in mixtures. Toxicol Appl Pharmacol; 167: 199–209.

Hamelin G, Charest-Tardif G, Truchon G *et al*. (2005) Physiologically based modeling of n-hexane kinetics in humans following inhalation exposure at rest and under physical exertion: impact on free 2,5-hexanedione in urine and on n-hexane in alveolar air. J Occup Environ Hyg; 2: 86–97.

Johanson G. (1986) Physiologically based pharmacokinetic modeling of inhaled 2-butoxyethanol in man. Toxicol Lett; 34: 23–31.

Johanson G, Boman A. (1991) Percutaneous absorption of 2-butoxyethanol vapour in human subjects. Br J Ind Med; 48: 788–92.

Jones K, Cocker J. (2003) A human exposure study to investigate biological monitoring methods for 2-butoxyethanol. Biomarkers; 8: 360–70.

Jongeneelen FJ, Anzion RBM, Henderson PT. (1987a) Determination of hydroxylated metabolites of polycyclic aromatic hydrocarbons in urine. J Chromatogr; 413: 227–32.

Jongeneelen FJ, Anzion RB, Scheepers PT *et al*. (1988) 1-Hydroxypyrene in urine as a biological indicator of exposure to polycyclic aromatic hydrocarbons in several work environments. Ann Occup Hyg; 32: 35–43.

Jongeneelen FJ, Hermans F, Anzion RBM *et al*. (1987b) Interindividual differences in hydroxylation of benzo(a)pyrene and pyrene in human liver preparations. Chapter 2 of PhD Thesis. University of Nijmegen-NL Nijmegen: Scientific Publishers. ISBN 90-9001458-6.

Kim D, Andersen ME, Pleil JD *et al*. (2007) Refined PBPK model of aggregate exposure to methyl tertiary-butyl ether. Toxicol Lett; 169: 222–35.

Kramer A, Below H, Bieber N *et al*. (2007) Quantity of ethanol absorption after excessive hand disinfection using three commercially available hand rubs is minimal and below toxic levels for humans. BMC Infect Dis; 11: 117.

Krewski D, Withey JR, Ku LF, Andersen ME. (1994) Applications of physiologic pharmacokinetic modeling in carcinogenic risk assessment. Environ Health Perspect; 102 (Suppl. 11): 37–50.

Leavens TL, Borghoff SJ. (2009) Physiologically based pharmacokinetic model of methyl tertiary butyl ether and tertiary butyl alcohol dosimetry in male rats based on binding to alpha2u-globulin. Toxicol Sci; 109: 321–35.

Levitt DG. (2002) PKQuest: a general physiologically based pharmacokinetic model. Introduction and application to propranolol. BMC Clin Pharmacol; 2: 5.

Licata AC, Dekant W, Smith CE *et al*. (2001) A physiologically based pharmacokinetic model for methyl tert-butyl ether in humans: implementing sensitivity and variability analyses. Toxicol Sci; 62: 191–204.

Ligocka D, Lison D, Haufroid V. (2003) Contribution of CYP2E1 to N-methylpyrrolidone metabolism. Arch Toxicol; 77: 261–6.

Luecke RH, Pearce BA, Wosilait WD *et al*. (2008) Windows based general PBPK/PD modeling software. Comput Biol Med; 38: 962–78.

Luukkanen L, Mikkola J, Forsman T *et al*. (2001) Glucuronidation of 1-hydroxypyrene by human liver microsomes and human UDP-glucuronosyltransferases UGT1A6, UGT1A7, and UGT1A9: development of a high-sensitivity glucuronidation assay for human tissue. Drug Metab Dispos; 29: 1096–101.

McCarley KD, Bunge AL. (1998) Physiologically relevant one-compartment pharmacokinetic models for skin. 1. Development Of models. J Pharm Sci; 87: 1264.

McCarley KD, Bunge AL. (2000) Physiologically relevant two-compartment pharmacokinetic models for skin. J Pharm Sci; 89: 1212–35.

Medinsky MA, Singh G, Bechtold WE *et al*. (1990) Disposition of three glycol ethers administered in drinking water to male F344/N rats. Toxicol Applied Pharmacol; 102: 443–55.

Meulenberg CJW, Vijverberg HPM. (2000) Emperical relations predicting human and rat tissue:air partition coefficients of volatile organic compounds. Toxicol Appl Pharmacol; 165: 206–21.

Perbellini L, Brugnone F, Caretta D *et al*. (1985) Partition coefficients of some industrial aliphatic hydrocarbons (C5-C7) in blood and human tissues. Br J Ind Med; 42: 162–7.

Perbellini L, Brugnone F, Cocheo V *et al*. (1986) Identification of the n-heptane metabolites in rat and human urine. Arch Toxicol; 58: 229–34.

Peyret T, Poulin P, Krishnan KA. (2010) Unified algorithm for predicting partition coefficients for PBPK modeling of drugs and environmental chemicals. Toxicol Appl Pharmacol; 249: 197–207.

Poet TS, Kirman CR, Bader M *et al*. (2010) Quantitative risk analysis for N-methyl pyrrolidone using physiologically based pharmacokinetic and benchmark dose modeling. Toxicol Sci; 113: 468–82.

Poulin P, Theil FP. (2002) Prediction of pharmacokinetics prior to in vivo studies. II. Generic physiologically based pharmacokinetic models of drug disposition. J Pharm Sci; 91: 1358–70.

Ramsey JC, Andersen ME. (1984) A physiologically based description of the inhalation pharmacokinetics of styrene in rats and humans. Toxicol Appl Pharmacol; 73: 159–75.

Reddy MB, McCarley KD, Bunge AL. (1998) Physiologically relevant one-compartment pharmacokinetic models for skin. 2. Comparison of models when combined with a systemic pharmacokinetic model. J Pharm Sci; 87: 482–90.

Reddy MB, Looney RJ, Utell MJ *et al*. (2007) Modeling of human dermal absorption of octamethylcyclotetrasiloxane (D(4)) and decamethylcyclopentasiloxane (D(5)). Toxicol Sci; 99: 422–31.

Rossbach B, Kegel P, Letzel S. (2010) Effects of an experimental exposure to 500 PPM nheptane on levels of n-haptene and its metabolites in blood. Poster Int Symposium BioMonitoring, 6/8 sept 2010. Helsinki, Finland: FIOH.

RSC. (2010) OpenEye, ChemSpider Database. Building community for chemists. Available at http://www.chemspider.com/.

Spaan S, Fransman W, Warren N *et al*. (2010) Variability of biomarkers in volunteer studies: the biological component. Toxicol Lett; 198: 144–51.

Strickland P, Kang D, Sithisarankul P. (1996) Polycyclic aromatic hydrocarbon metabolites in urine as biomarkers of exposure and effect. Environ Health Perspect; 104 (Suppl. 5): 927–32. Review.

Szutowski MM, Rakoto JS. (2009) Multiplicity of n-heptane oxidation pathways catalyzed by cytochrome P450. J Biochem Mol Toxicol; 23: 287–94.

Tardif R, Droz PO, Charest-Tardif G *et al*. (2002) Impact of human variability on the biological monitoring of exposure to toluene: I. Physiologically based toxicokinetic modelling. Toxicol Lett; 134: 155–63.

Teeguarden JG, Waechter JM Jr, Clewell HJ 3rd *et al*. (2005) Evaluation of oral and intravenous route pharmacokinetics, plasma protein binding, and uterine tissue dose metrics of bisphenol A: a physiologically based pharmacokinetic approach. Toxicol Sci; 85: 823–38.

ten Berge W. (2009) A simple dermal absorption model: derivation and application. Chemosphere; 75: 1440–5.

Umulis DM, Gürmen NM, Singh P *et al*. (2005) A physiologically based model for ethanol and acetaldehyde metabolism in human beings. Alcohol; 35: 3–12. Review.

US-EPA. (2006) Exposure Related Dose Estimating Model (ERDEM). Available at http://www.epa.gov. Accessed 7 September 2011.

US-EPA. (2009) Episuite 4.0. Estimation Program Interface (EPI) Suite. USEPA. Available at http://www.epa.gov/opptintr/exposure/pubs/episuitedl.htm. Accessed 7 September 2011.

van der Merwe D, Brooks JD, Gehring R *et al*. (2006) A physiologically based pharmacokinetic model of organophosphate dermal absorption. Toxicol Sci; 89: 188–204.

van de Waterbeemd H, Gifford E. (2003) ADMET in silico modelling: towards prediction paradise? Nat Rev Drug Discov; 2: 192–204.

Van Rooij JG, Van Lieshout EM, Bodelier-Bade MM *et al*. (1993) Effect of the reduction of skin contamination on the internal dose of creosote workers exposed to polycyclic aromatic hydrocarbons. Scand J Work Environ Health; 19: 200–7.

Willmann S, Lippert J, Schmitt W. (2005) From physicochemistry to absorption and distribution: predictive mechanistic modelling and computational tools. Expert Opin Drug Metab Toxicol; 1: 159–68.

Wilschut A, ten Berge WF, Robinson PJ *et al*. (1995) Estimating skin permeation. The validation of five mathematical skin permeation models. Chemosphere; 30: 1275–96.

Woodard HQ, White DR. (1986) The composition of body tissues. Br J Radiol; 59: 1209–18.

Yu LX, Amidon GL. (1999) A compartmental absorption and transit model for estimating oral drug absorption. Int J Pharm; 186: 119–25.

Zorin S, Kuylenstierna F, Thulin H. (1999) In vitro test of nicotine's permeability through human skin. Risk evaluation and safety aspects. Ann Occup Hyg; 1999: 405–13.